

# NONEQUILIBRIUM TUNNELING EFFECTS OF INTERACTING HUBBARD–ANDERSON IMPURITIES

*P. I. Arseev*<sup>a\*</sup>, *N. S. Maslova*<sup>b</sup>, *V. I. Panov*<sup>b</sup>, *S. V. Savinov*<sup>b</sup>

<sup>a</sup> *Lebedev Physical Institute of Russian Academy of Sciences  
119991, Moscow, Russia*

<sup>b</sup> *Moscow State University  
119899, Moscow, Russia*

Submitted 20 April 2001

Nonequilibrium interaction effects of two Hubbard–Anderson impurities have been experimentally studied by means of STM/STS methods and theoretically analyzed using a self-consistent approach based on the Keldysh formalism.

PACS: 72.15.-v

Impurity states at surfaces and interfaces of semiconductors can strongly modify the local electronic structure. As the system size decreases, the correct understanding of localized state properties becomes more and more important. The interaction between impurities must also be taken into account as the impurity concentration increases. If the distance between impurities is of the order of the localization radius, sufficiently strong correlation effects arise that modify the tunneling conductivity. The electronic structure of such complexes can be tuned by an external electric field. These effects are believed to determine electronic properties of semiconductor nanostructures in the future. However, local effects caused by the interaction of two impurity states near the surface are not well examined at present. A powerful tool for studying the local electronic structure is the scanning tunneling spectroscopy (STS) combined with the scanning tunneling microscopy (STM) imaging. In the present work, the electronic structure of localized impurity states formed by a pair of impurity Si atoms separated by 3 nm at the (110) GaAs surface are studied by the STM/STS methods.

The samples under investigation are GaAs single crystals doped with compensating impurities Si and Zn with the respective concentrations  $5 \cdot 10^{18} \text{ cm}^{-3}$  and  $2 \cdot 10^{19} \text{ cm}^{-3}$ . All measurements were carried out at

4.2 K with a home-built low-temperature STM with an *in situ* cleavage mechanism [1]. After the crystal was cleaved along the (110) plane, two Si atoms with the spatial separation about 3 nm were chosen as the object of investigation. The separation distance is comparable to the visible localization radius of the Si impurity states, which is about 1–1.5 nm (Fig. 1a). A high doping level accounts for a nonuniform Coulomb potential in the sample. This is one of the reasons why the initial electronic states of the observed atoms are not equivalent. The scanned area was 10 nm  $\times$  10 nm and within this area, the tunneling conductivity  $(dI/dV)/(I/V)$  was measured with the spatial step 0.25 nm.

In the experimentally observed spatial distribution of the local tunneling conductivity, one can distinguish a two-fold switching on and off for each of the atomic «*a*» and «*b*» states upon changing the tunneling bias within the semiconductor band gap (visible as the dark stripe in Fig. 1). After switching on, the excess tunneling conductivity occurs in the vicinity of each of these atoms in a bias range about 0.65 eV, which is much greater than the level width of the localized state. At the same time, the transition from the «dark» state to the «light» one occurs within the bias change range  $\approx 0.15$  eV, which is comparable to the energy level width of the localized state.

The map view of the tunneling conductivity allows analyzing the evolution of the local density of states (LDOS) near each impurity atom. At zero applied bias,

---

\*E-mail: ars.@pli.ac.ru

**Fig. 1.** STM images (right panel) and the map view of the normalized tunneling conductivity measured along the direction  $x$  depicted on the STM topography images (left panel).  $a$  — an isolated Si impurity, scan area 5.8 nm, bias range from +2.5 V to  $-2$  V,  $b$  — two interacting Si impurities, scan area 10 nm, bias range from +2.5 V to  $-2$  V

atom « $a$ » forms a bright area of the enhanced tunneling conductivity and remains «switched on» in bias range from  $-0.2$  V to  $+0.4$  V. Atom « $b$ » is invisible at  $V \approx 0$ . In the bias range from  $+0.4$  V to  $+0.7$  V, the tunneling conductivity decreases in the vicinity of atom « $a$ » (dark area). The next switching on of this atom occurs

at  $+0.7$  V and a bright spot of the enhanced tunneling conductivity is observed up to  $+1.3$  V.

The enhanced tunneling conductivity near atom « $b$ » is also observed in two separated bias ranges: from  $+0.1$  V to  $+0.5$  V and at the same polarity from  $+0.6$  V to  $+1.2$  V. In Fig. 2, two experimentally obtained

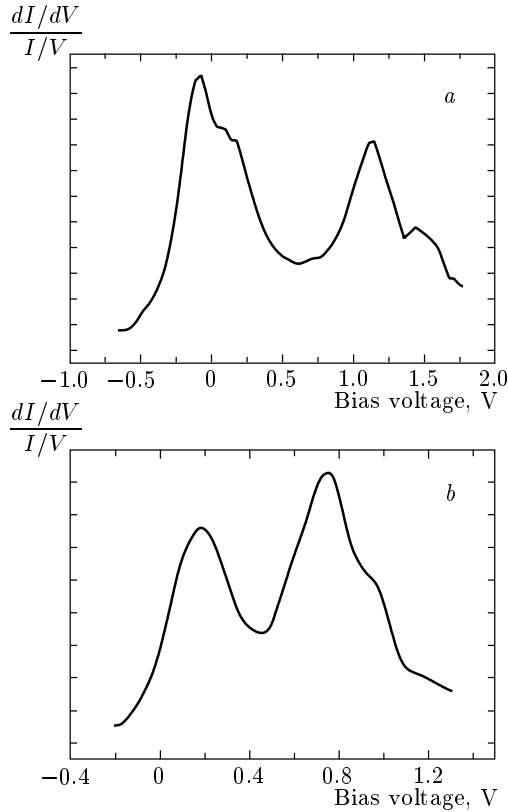


**Fig. 2.** The normalized conductance  $(dI/dV)/(I/V)$  measured within the semiconductor band gap in the vicinity of impurity atoms: *a* — the STM tip is placed over the «*a*» atom on Fig. 1*b*; *b* — the STM tip is placed over the «*b*» atom in Fig. 1*b*

$(dI/dV)/(I/V)$  curves are shown for two different positions of the STM tip: above atom «*a*» and above atom «*b*».

Because such effects have not been observed for an isolated impurity, a natural question is to what extent the interaction between the two impurities modifies the kinetic processes. To answer this question, we suggest a self-consistent theoretical analysis of the local tunneling conductivity behavior in the vicinity of two interacting Anderson impurities on a semiconductor surface [2]. In the Anderson model [3], an individual impurity state is characterized by the following parameters: the bare impurity electron level  $\varepsilon_0$ , the on-site Coulomb repulsion of localized electrons  $U$ , and the level broadening  $\Gamma$  caused by the hybridization with continuum states. It is known that nontrivial effects occur in the Anderson model if the on-site Coulomb repulsion is sufficiently strong. Because the experimentally observed localization radius of Si impurity states at the GaAs surface is of the order of 1 nm, the estimated value of the Hub-

bard energy is about 0.5–1 eV. It must be mentioned that although the Si atoms in the bulk GaAs are known to form a shallow impurity state with binding energies about 6 meV at low doping levels, the situation is different near the surface in the presence of the STM tip. It was experimentally observed by many authors (see, e.g. [4–6]) that the band bending induced by the surface and by the STM tip can considerably change the position of the Si impurity level relative to the conduction band edge. Numerous STM images (see references above) show that the localization radius of the Si atom state is about 1–1.5 nm. In highly doped crystals, in addition the electronic state of any particular atom can be strongly modified by the presence of neighboring dopant atoms.

The electron transport through a single Anderson impurity in the Coulomb blockade and the Kondo regime has been studied experimentally and is still under theoretical investigation [7–13]. However, most of the authors concentrated on the weak tunneling coupling, when the tunnel junction is used only as a probe without affecting the impurity states [9]. Therefore, the tunneling conductivity through the Anderson impurity is usually supposed to be determined by the equilibrium impurity density of states. In the Coulomb blockade regime of tunneling through an impurity or a quantum dot, the influence of the tunneling current on the impurity (dot) spectrum is neglected [11]. The impurity charge therefore takes discrete values;  $n_\sigma$  and  $n_{-\sigma}$  can be equal only to 0 or 1. The width of the tunneling conductivity peak in the Coulomb blockade regime is determined by the sum of relaxation rates and cannot achieve (without destroying this regime) the experimentally observed anomalously large values  $\approx 0.65$  eV even at room temperatures. As the tunneling coupling increases, the impurity charge is no longer a discrete value and one must consider impurity electron filling numbers (which now become continuous variables) determined from the kinetic equations.

We note that the coupling to the leads in the Kondo regime modifies the impurity spectrum, but charge fluctuations are suppressed because the initial impurity level lies deep below the Fermi level [14]. In the equilibrium case, the electron filling numbers  $n_\sigma$  and  $n_{-\sigma}$  satisfy the relation

$$n_\sigma + n_{-\sigma} = 1.$$

Spin fluctuations dominate in this case because the impurity state is always single occupied. This requires the following relations between the parameters of the Anderson model:  $-\varepsilon_0 \gg \Gamma$  and  $\varepsilon_0 + U \gg \Gamma$ . The Kondo resonance then contributes to the zero-bias anomaly of

the tunneling conductivity. But the contribution of the Kondo effect to the tunneling conductivity dependence on the applied voltage becomes almost negligible when the applied bias exceeds a typical energy value determined by the Kondo temperature (small compared to  $\varepsilon_0$  and  $\Gamma$ ) (see [15, 16]). When the applied bias increases (decreases) to the impurity energy level, the Kondo resonance is destroyed.

In the present work, we are interested in the tunneling conductivity behavior in a wide bias range from +2.5 V to -2 V (while the typical value of the Kondo temperature is less than 1 meV). The adopted parameters of the model correspond to the mixed-valence regime,  $\varepsilon \approx \Gamma$  or  $\varepsilon + U \approx \Gamma$  (although  $U \gg \Gamma$ ). This choice of the set of parameters is more adequate for our analysis of the anomalies in the tunneling conductivity behavior observed experimentally in a wide bias range  $V$  comparable to  $U$  and  $V \geq \varepsilon_0$ . Under all these conditions, the Kondo effect does not reveal itself in the tunneling characteristics, although spin asymmetry of the electron filling numbers occurs in particular bias ranges.

As the applied bias is increased, nonequilibrium processes start playing a significant role, especially at low temperatures. Nonequilibrium effects in the tunneling conductivity spectra of metallic nanoparticles have been considered by Agam and co-authors [17]. In this work, changes of the energy of an excited single electron state are caused at large applied bias by different nonequilibrium occupancy configurations of other single electron states. It was assumed that the electron spectrum of a nanoparticle consists of many levels and the level spacing is smaller than the applied bias. But the filling numbers of each level are equal to either 0 or 1. Different random configurations of the electron occupation result in fluctuations of the Coulomb interaction energy. However, continuous changes in nonequilibrium electron filling numbers caused by kinetic processes were not taken into account.

In the present work, the nonequilibrium charge distribution due to tunneling processes and the effect of the tunneling bias voltage on the impurity state energy values are taken into account. Nonequilibrium electron filling numbers on the Hubbard-Anderson impurities are calculated from a self-consistent system of kinetic equations based on the Keldysh diagram technique [18]. At the final stage of calculations, the Coulomb interaction of localized electrons is treated self-consistently in the mean-field approximation. It is shown that with increasing the tunneling bias, two states with different energies for opposite-spin electrons can appear at each impurity: the transition from the «paramagnetic»

regime to the «magnetic» one can occur. The inverse transition from the «magnetic» to the «paramagnetic» state can also occur with further increasing the tunneling bias. We have also determined the conditions under which the transition to the magnetic state is enhanced by the interaction between the two Anderson impurities. We found that the impurity interaction results in a redistribution of localized non-equilibrium charges and can lead to pinning of the impurity levels near the Fermi level of each electrode and to the mutual attraction of the energy levels of different impurities in particular ranges of the applied bias.

We consider a theoretical model with two interacting Anderson impurities. The STM tip is supposed to be positioned above one of the impurity atoms (atom «a»). The Hamiltonian of the model is given by

$$\hat{H} = \hat{H}_0 + \hat{H}_{tun} + \hat{H}_{int} + \hat{H}_{imp}, \quad (1)$$

where

$$\begin{aligned} \hat{H}_0 = & \sum_{\mathbf{k},\sigma} (\varepsilon_{\mathbf{k}} - \mu) c_{\mathbf{k},\sigma}^+ c_{\mathbf{k},\sigma} + \\ & + \sum_{\mathbf{p},\sigma} (\varepsilon_{\mathbf{p}} - \mu - eV) c_{\mathbf{p},\sigma}^+ c_{\mathbf{p},\sigma} \end{aligned} \quad (2)$$

describes noninteracting electrons in the two electrodes,  $(\mathbf{k}, \sigma)$  for the tip and  $(\mathbf{p}, \sigma)$  for the example.

The part  $\hat{H}_{imp}$  corresponds to the impurity states and takes the Hubbard repulsion into account,

$$\begin{aligned} \hat{H}_{imp} = & \varepsilon_a \sum_{\sigma} a_{\sigma}^+ a_{\sigma} + \frac{U_a}{2} \sum_{\sigma} n_{\sigma}^a n_{-\sigma}^a + \\ & + \varepsilon_b \sum_{\sigma} b_{\sigma}^+ b_{\sigma} + \frac{U_b}{2} \sum_{\sigma} n_{\sigma}^b n_{-\sigma}^b. \end{aligned} \quad (3)$$

Here,  $n_{\sigma}^a = a_{\sigma}^+ a_{\sigma}$ ,  $a_{\sigma}$  destroys an impurity «a» electron with the spin  $\sigma$ ,  $n_{\sigma}^b = b_{\sigma}^+ b_{\sigma}$ ,  $b_{\sigma}$  destroys an impurity «b» electron with the spin  $\sigma$ , and  $\varepsilon_a$  and  $\varepsilon_b$  are the energy levels of impurities «a» and «b» (they depend on the bias  $V$  in general).

The part  $\hat{H}_{int}$  describes the interaction between the impurity states,

$$\hat{H}_{int} = T \sum_{\sigma} (a_{\sigma}^+ b_{\sigma} + \text{h.c.}), \quad (4)$$

and  $\hat{H}_{tun}$  is responsible for tunneling transitions from the impurity states to each electrode (tip or substrate),

$$\begin{aligned} \hat{H}_{tun} = & T_{\mathbf{p},a} \sum_{\mathbf{p},\sigma} (c_{\mathbf{p},\sigma}^+ a_{\sigma} + \text{h.c.}) + \\ & + T_{\mathbf{p},b} \sum_{\mathbf{p},\sigma} (c_{\mathbf{p},\sigma}^+ b_{\sigma} + \text{h.c.}) + T_{\mathbf{k},a} \sum_{\mathbf{k},\sigma} (c_{\mathbf{k},\sigma}^+ a_{\sigma} + \text{h.c.}). \end{aligned} \quad (5)$$

Nonequilibrium effects in the tunneling current and conductivity are naturally described by the Keldysh diagram technique ([19], see also the recent paper [16]).

The tunneling current is determined as [19]

$$I(V) = \sum_{\mathbf{k}, \sigma} \int d\omega T_{\mathbf{k}\alpha} (G_{\alpha\mathbf{k}}^{\sigma<} - G_{\mathbf{k}\alpha}^{\sigma<}). \quad (6)$$

The functions  $G_{\alpha\mathbf{k}}^{\sigma<}$  can be obtained from the kinetic equations, which in the Keldysh formalism are of the general form

$$(\widehat{G}_0^{-1} - \widehat{G}_0^{*-1})\widehat{G}^< = (\widehat{\Sigma}\widehat{G})^< - (\widehat{G}\widehat{\Sigma})^<, \quad (7)$$

where  $\widehat{\Sigma}$  usually includes all the interactions; in our case, however,  $\widehat{\Sigma}$  is determined only by the tunneling coupling to the leads and by the interaction between the impurities. Therefore, the elements of  $\widehat{\Sigma}$  simply reduce to the corresponding nonzero parameters  $T_{\alpha,\beta}$  ( $\alpha, \beta = a, b, \mathbf{k}, \mathbf{p}$ ). It is reasonable to use the approximation in which the strongest interaction of the considered model — the on-site Coulomb repulsion  $U$  — is included in  $G_0$ . At this stage, it is not necessary to consider the details of any particular approximation for treating  $U$ .

With the help of the kinetic equations, tunneling current (6) can be transformed to the form

$$I_\sigma(V) = -4\gamma_{\mathbf{k}} \times \int \text{Im} G_{a,a}^{R\sigma}(\omega) (n_a^\sigma(\omega) - n_{\mathbf{k}}^0(\omega - eV)) d\omega, \quad (8)$$

where  $n_{\mathbf{k}}^0(\omega)$  is the equilibrium filling number for the metallic tip,  $G_{a,a}^{R\sigma}(\omega, V)$  is the exact retarded Green's function of the impurity «a» state,  $n_a^\sigma(\omega)$  is the exact impurity filling number, and the tunneling rate  $\gamma_{\mathbf{k}}$  is one of the set of kinetic coefficients determined by

$$\begin{aligned} \gamma_{\mathbf{k}}(\omega) &= |T_{\mathbf{k}\alpha}|^2 \nu_{\mathbf{k}}(\omega), & \gamma_b(\omega) &= |T_{\mathbf{p}b}|^2 \nu_{\mathbf{p}}(\omega), \\ \gamma_a(\omega) &= |T_{\mathbf{p}a}|^2 \nu_{\mathbf{p}}(\omega), & \Gamma &= \gamma_a + \gamma_b + \gamma_{\mathbf{k}}, \end{aligned} \quad (9)$$

where

$$\nu_{\mathbf{k}}(\omega) = -\frac{1}{\pi} \sum_{\mathbf{k}} \text{Im} G^R(k, \omega)$$

is the density of states in the metallic tip and

$$\nu_{\mathbf{p}}(\omega) = -\frac{1}{\pi} \sum_{\mathbf{p}} \text{Im} G^R(\mathbf{p}, \omega)$$

is the substrate density of states.

In Eq. (8) and in what follows, we use the standard approximation with the filling numbers  $n_{\mathbf{k}}^0(\omega)$  and

$n_{\mathbf{p}}^0(\omega)$  for the continuum states of the banks unperturbed by the tunneling processes, which yields

$$\begin{aligned} G_{\mathbf{k},\mathbf{k}}^<(\omega) &= -2in_{\mathbf{k}}^0(\omega) \text{Im} G_{\mathbf{k},\mathbf{k}}^{R}, \\ G_{\mathbf{p},\mathbf{p}}^<(\omega) &= -2in_{\mathbf{p}}^0(\omega) \text{Im} G_{\mathbf{p},\mathbf{p}}^{R}. \end{aligned} \quad (10)$$

Equation (8) shows that the problem is reduced to finding the exact nonequilibrium filling number  $n_a^\sigma$ . This problem can be solved using Eqs. (7) for  $G_{aa}^<, G_{bb}^<$ , and  $G_{ab}^<$  in the stationary case,

$$0 = \frac{\partial}{\partial t} G_{aa}^< = T(G_{ba}^< - G_{ab}^<) + 2\gamma_a \text{Im} G_{aa}^{\sigma R} (n_a^\sigma - n_{\mathbf{p}}^0) + 2\gamma_{\mathbf{k}} \text{Im} G_{aa}^{\sigma R} (n_a^\sigma - n_{\mathbf{k}}^0), \quad (11)$$

$$0 = \frac{\partial}{\partial t} G_{bb}^< = T(G_{ab}^< - G_{ba}^<) + 2\gamma_b \text{Im} G_{bb}^{\sigma R} (n_b^\sigma - n_{\mathbf{p}}^0), \quad (12)$$

$$0 = \frac{\partial}{\partial t} G_{ab}^< = -R_{ab}^{-1} G_{ab}^< + T(G_{bb}^< - G_{aa}^<) + 2(\gamma_a G_{ab}^{\sigma A} - \gamma_b G_{ab}^{\sigma R}) n_{\mathbf{p}}^0 + 2\gamma_{\mathbf{k}} G_{ab}^{\sigma A} n_{\mathbf{k}}^0, \quad (13)$$

$$0 = \frac{\partial}{\partial t} G_{ba}^< = R_{ab}^{-1} G_{ba}^< + T(G_{aa}^< - G_{bb}^<) + 2(\gamma_b G_{ba}^{\sigma A} - \gamma_a G_{ba}^{\sigma R}) n_{\mathbf{p}}^0 - 2\gamma_{\mathbf{k}} G_{ba}^{\sigma R} n_{\mathbf{k}}^0, \quad (14)$$

where we use the notation

$$R_{ab}^{-1} = G_{0a}^{R-1} - G_{0b}^{A-1} - i\Gamma. \quad (15)$$

For  $n_a^\sigma(\omega)$  and  $n_b^\sigma(\omega)$ , we then have

$$\begin{aligned} \gamma_{\mathbf{k}} \text{Im} G_{aa}^{\sigma R}(\omega) (n_a^\sigma(\omega) - n_{\mathbf{k}}^0(\omega)) &= \\ &= -[\gamma_a \text{Im} G_{aa}^{\sigma R}(\omega) (n_a^\sigma(\omega) - n_{\mathbf{p}}^0(\omega)) + \\ &+ \gamma_b \text{Im} G_{bb}^{\sigma R}(\omega) (n_b^\sigma(\omega) - n_{\mathbf{p}}^0(\omega))] , \\ \eta^\sigma \text{Im} G_{aa}^{\sigma R}(\omega) n_a^\sigma(\omega) - \text{Im} G_{bb}^{\sigma R}(\omega) n_b^\sigma(\omega) &= \\ &= \gamma_b \text{Im} G_{bb}^{\sigma R}(\omega) (n_b^\sigma(\omega) - n_{\mathbf{p}}^0(\omega)) + \\ &+ n_{\mathbf{p}}^0(\omega) T(\gamma_a \text{Im}(R_{ab}^\sigma G_{ab}^{\sigma A}) - \gamma_b \text{Im}(R_{ab}^\sigma G_{ab}^{\sigma R})) + \\ &+ n_{\mathbf{k}}^0(\omega) T \gamma_{\mathbf{k}} \text{Im}(R_{ab}^\sigma G_{ab}^{\sigma A}), \end{aligned} \quad (16)$$

where

$$\eta^\sigma = T^2 \text{Im} R_{ab}^\sigma$$

and where  $n_{\mathbf{p}}^0(\omega)$  and  $n_{\mathbf{k}}^0(\omega - eV)$  are the respective equilibrium filling numbers of the substrate and the metallic tip states.

It must be noted that no particular approximation for treating the Coulomb interaction has been used until now. If we use the mean-field approximation, which

is suitable for the mixed-valence regime, for decoupling the on-site Coulomb interaction, we obtain

$$\begin{aligned}
 R_{ab}^\sigma &= \frac{1}{(\tilde{\varepsilon}_a^\sigma - \tilde{\varepsilon}_b^\sigma) - i(\gamma_{\mathbf{k}} + \gamma_a + \gamma_b)}, \\
 G_{aa}^{\sigma R}(\omega) &= \frac{\omega - \tilde{\varepsilon}_b^\sigma + i\gamma_b}{(\omega - \tilde{\varepsilon}_b^\sigma + i\gamma_b)(\omega - \tilde{\varepsilon}_a^\sigma + i(\gamma_a + \gamma_{\mathbf{k}})) - T^2}, \\
 G_{bb}^{\sigma R}(\omega) &= \frac{\omega - \tilde{\varepsilon}_a^\sigma + i(\gamma_a + \gamma_{\mathbf{k}})}{(\omega - \tilde{\varepsilon}_b^\sigma + i\gamma_b)(\omega - \tilde{\varepsilon}_a^\sigma + i(\gamma_a + \gamma_{\mathbf{k}})) - T^2}, \\
 G_{ab}^{\sigma R}(\omega) &= \frac{T}{(\omega - \tilde{\varepsilon}_b^\sigma + i\gamma_b)(\omega - \tilde{\varepsilon}_a^\sigma + i(\gamma_a + \gamma_{\mathbf{k}})) - T^2}.
 \end{aligned} \tag{17}$$

In the mean-field approximation, the impurity energies depend on the applied bias  $V$  both directly through the external field in the contact area (which changes the «bare» impurity level) and indirectly through the Coulomb interaction of the nonequilibrium electron density,

$$\begin{aligned}
 \tilde{\varepsilon}_a^\sigma &= \varepsilon_a + \alpha V + U_a \langle n_a^{-\sigma} \rangle, \\
 \tilde{\varepsilon}_b^\sigma &= \varepsilon_b + \beta V + U_b \langle n_b^{-\sigma} \rangle.
 \end{aligned} \tag{18}$$

The coefficients  $\alpha$  and  $\beta$  ( $\alpha, \beta < 1$ ) approximately describe the potential drop between the semiconductor substrate and the impurity. (If one deals with the Coulomb blockade regime, the electron filling numbers  $\langle n^\sigma \rangle$  are set equal to 0 or 1, because the hybridization with the lead states is neglected.)

For simplicity, the indirect interaction between the impurities through the semiconductor band states is not included in the presented results. This interaction can be easily taken into account but it does not lead to any new qualitative changes of the tunneling conductivity behavior.

Now the main point is that the nonequilibrium electron filling numbers for impurity atoms « $a$ » and « $b$ » must satisfy the self-consistency condition

$$\begin{aligned}
 n_a^\sigma &= \int d\omega n_a^\sigma(\omega) \text{Im} G_{aa}^R(\omega), \\
 n_b^\sigma &= \int d\omega n_b^\sigma(\omega) \text{Im} G_{bb}^R(\omega),
 \end{aligned} \tag{19}$$

where  $n_a^\sigma(\omega)$  and  $n_b^\sigma(\omega)$  are determined by stationary equations (16). Equations (19) can be rewritten as

$$\begin{aligned}
 n_a^\sigma &= n_{\mathbf{p}}^\sigma(a) + \\
 &+ \frac{\gamma_{\mathbf{k}}(\gamma_b + \eta_\sigma)(n_{\mathbf{k}}^\sigma(a) - n_{\mathbf{p}}^\sigma(a)) + \gamma_b \Gamma_{ab}}{(\gamma_{\mathbf{k}} + \gamma_a)(\gamma_b + \eta_\sigma) + \gamma_b \eta_\sigma},
 \end{aligned} \tag{20}$$

$$\begin{aligned}
 n_b^\sigma &= n_{\mathbf{p}}^\sigma(b) + \\
 &+ \frac{\gamma_{\mathbf{k}} \eta_\sigma (n_{\mathbf{k}}^\sigma(a) - n_{\mathbf{p}}^\sigma(a)) - (\gamma_a + \gamma_{\mathbf{k}}) \Gamma_{ab}}{(\gamma_{\mathbf{k}} + \gamma_a)(\gamma_b + \eta_\sigma) + \gamma_b \eta_\sigma},
 \end{aligned} \tag{21}$$

where

$$\begin{aligned}
 \Gamma_{ab} &= T \gamma_{\mathbf{k}} \times \\
 &\times \int \text{Im}(R_{ab} G_{ab}^{R\sigma}(\omega))(n_{\mathbf{k}}(\omega) - n_{\mathbf{p}}(\omega)) d\omega,
 \end{aligned} \tag{22}$$

$$n_{\mathbf{p}(\mathbf{k})}^\sigma(a) = \int d\omega n_{\mathbf{p}(\mathbf{k})}^0(\omega) \text{Im} G_{aa}^R(\omega) \tag{23}$$

(with the Fermi level for  $n_{\mathbf{k}}$  shifted by  $eV$  from the Fermi level for  $n_{\mathbf{p}}$ ). For the equilibrium case,  $V = 0$  and  $n_a^\sigma = n_{\mathbf{p}}^\sigma(a) = n_{\mathbf{k}}^\sigma(a)$ .

Solving Eqs. (16) for  $n_a^\sigma(\omega)$ , we can rewrite the tunneling current in Eq. (8) in the final form

$$\begin{aligned}
 I_\sigma(V) &= \frac{\gamma_{\mathbf{k}}(\gamma_b + \eta_\sigma)}{(\gamma_a + \gamma_{\mathbf{k}})(\gamma_b + \eta_\sigma) + \gamma_b \eta_\sigma} \times \\
 &\times \int \left[ \left( \gamma_a + \frac{\gamma_b \eta_\sigma}{\gamma_b + \eta_\sigma} \right) \text{Im} G_{a,a}^{R\sigma}(\omega, V) + \right. \\
 &\left. + T \frac{\gamma_b \gamma_{\mathbf{k}}}{\gamma_b + \eta_\sigma} \text{Im}(R_{ab} G_{ab}^{A\sigma}(\omega, V)) \right] \times \\
 &\times (n_{\mathbf{p}}^0(\omega) - n_{\mathbf{k}}^0(\omega - eV)) d\omega,
 \end{aligned} \tag{24}$$

where the self-consistent values for  $n_a^\sigma$  and  $n_b^\sigma$  are inserted in  $G_{aa}^R$ ,  $G_{ab}^R$ , and  $R_{ab}$  for each value of the bias  $V$ . As expected, the tunneling current depends only on the difference of the electron distribution functions of the electrodes. The first term of the above expression for the tunneling current describes the renormalization of the relaxation rate by the interaction with the neighboring impurity atom « $b$ »,

$$\gamma_a \longrightarrow \gamma_a + \frac{\gamma_b \eta_\sigma}{\gamma_b + \eta_\sigma}. \tag{25}$$

If the interaction is absent,  $T = 0$ , then  $\eta = 0$  and the usual form of the tunneling current through the impurity localized state is restored. The second term is responsible for the charge redistribution between the interacting impurity atoms. As a consequence of this charge redistribution, we obtain that the tunneling conductivity (see (24)) is no longer simply proportional to the impurity density of states. These complications make the investigation of the tunneling current through a multi-channel system with the interaction between different channels much more difficult (see, e.g., [20]).

In what follows, the interaction between the impurities is chosen (in accordance with the experimental situation) not greater than the tunneling rates.

This implies that the equilibrium level splitting (see Eqs. (17)) is not resolved via level broadening. In kinetic processes, however, the interaction considerably modifies the charge distribution. The opposite situation, with the zero-bias conductivity determined by the exact equilibrium spectrum of the two-site complex, was recently analyzed in [13].

We emphasize that Eq. (6) is exact and is valid in any case, irrespective of the approximations used in calculating  $\text{Im} G_a^R$  and  $n_a$ . Equations (19)–(24) can be applied to any regime, including the Coulomb blockade regime, with the proper choice of the retarded Green's function and the  $R_{ab}$  function. However, as noted in the introduction, in the present paper we are mainly interested in the mixed valence regime  $\varepsilon \approx \gamma$  or  $\varepsilon + U \approx \gamma$  and  $U \gg \gamma$ , and we therefore use mean-field equations (17) for numerical calculations of the tunneling conductivity.

The tunneling conductivity enhancement can usually be observed at the tunneling bias voltage such that

$$|\varepsilon_a^{\pm\sigma}(V) - E_F^t| < \Gamma$$

or

$$|\varepsilon_a^{\pm\sigma}(V) - E_F^s| < \Gamma.$$

But it is very important to note that any increase of the LDOS in the energy interval

$$E_F - eV < \varepsilon < E_F$$

with changing of the applied bias  $V$  leads to an enhancement of the tunneling conductivity at  $eV$ . This increase of the LDOS for an interacting system is not necessarily related to crossing a single electron level  $\varepsilon$  by the shifted Fermi level  $E_F - eV$ .

The analysis of the proposed model allows describing different possible regimes of the tunneling conductivity behavior in the vicinity of impurity atoms in a wide range of tunneling bias changes. In numerical calculations, we adopt  $\alpha \approx 0.3$  and  $\beta \approx 0.1$  in Eq. (18).

1) If  $\gamma_{\mathbf{k}} \ll \gamma_a, \gamma_b$ , one of the impurity atoms (atom « $a$ ») can be in the «magnetic» state in a certain tunneling bias range. The transition from the «paramagnetic» regime to the «magnetic» one and vice versa can occur with changing of the applied voltage (Fig. 3a). This behavior leads to switching the « $a$ » atom «on» and «off» twice on spatially resolved local tunneling conductivity spectra (Fig. 3b), which are very similar to the STS experimental data shown in Fig. 2.

In addition, the energy levels are pinned in the vicinity of the Fermi level of one of the electrodes (tip or sample) while the bias voltage changes within an order  $U$  range.

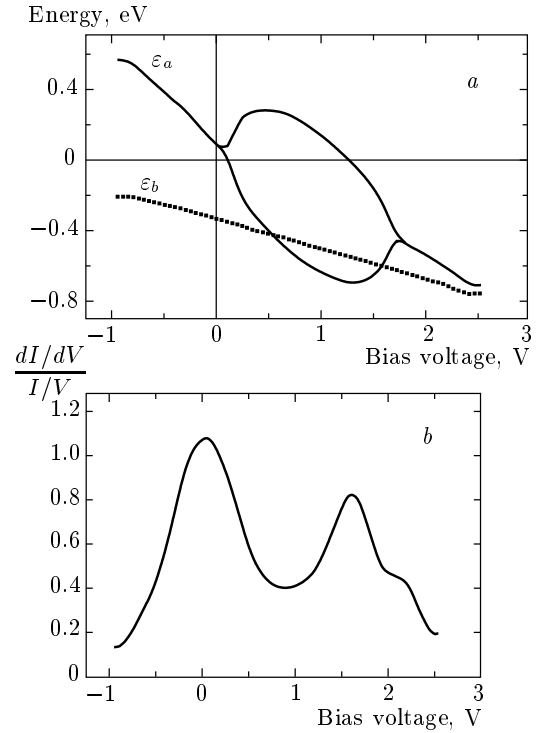


**Fig. 3.** A well pronounced two-fold structure of the tunneling conductivity with an increased peak width, very similar to the one observed in STS experiments. *a* — The dependence of the « $a$ » and « $b$ » atom energies on the applied bias  $V$ ; the parameter values are (in eV)  $\varepsilon_a^0 = -0.25$ ,  $\varepsilon_b^0 = -0.5$ ,  $U_a = 1.6$ ,  $U_b = 0.5$ ,  $\gamma_a = 0.2$ ,  $\gamma_b = 0.2$ ,  $\gamma_{\mathbf{k}} = 0.05$ ,  $\varepsilon_a = \varepsilon_a^0 - 0.3$  V,  $\varepsilon_b = \varepsilon_b^0 - 0.1$  V;  $T = 0.2$ ; solid lines correspond to  $\varepsilon_a^\sigma$  and  $\varepsilon_a^{-\sigma}$ , dotted line shows the mean value of  $\varepsilon_b = (1/2)(\varepsilon_b^\sigma + \varepsilon_b^{-\sigma})$  because atom « $b$ » is close to the paramagnetic state for this set of parameters. *b* — The normalized tunneling conductivity vs. the applied bias voltage

In the nonequilibrium case, where the tunneling bias is not zero, the interaction between atoms « $a$ » and « $b$ » can enhance the «magnetic» state and increase the difference between the energy values  $\varepsilon_{\sigma}$  and  $\varepsilon_{-\sigma}$  of the opposite-spin electrons localized on atom « $a$ ».

A detailed analysis of the tunneling bias range for which

$$|\varepsilon_a^{-\sigma}(V, n_a^\sigma) - E_F^s| < \Gamma$$

leads to the following conclusions.

If there is no interaction between the atoms (the bias range is such that  $|\varepsilon_a^{-\sigma}(V, n_a^\sigma) - E_F^s| < \Gamma$ ), the occupancy of the state  $\varepsilon_a^{-\sigma}(V, n_a^\sigma)$  grows and  $n_a^{-\sigma}(V)$  and  $\varepsilon_a^\sigma(V)$  increase; consequently,  $n_a^\sigma(V)$  and  $\varepsilon_a^{-\sigma}(V)$  decrease. The levels  $\varepsilon_a^{-\sigma}(V, n_a^\sigma)$  and  $\varepsilon_a^\sigma(V, n_a^{-\sigma})$  become closer and a sharp transition from the «magnetic» to the «paramagnetic» state occurs (Fig. 4b).

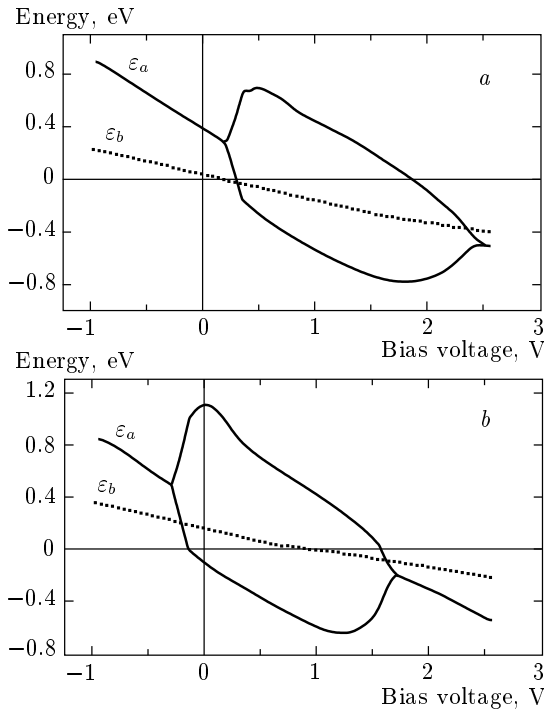


**Fig. 4.** The dependence of the «*a*» and «*b*» atom energies on the applied bias *V*. The parameter values are (in eV)  $\varepsilon_a^0 = -0.25$ ,  $\varepsilon_b^0 = -0.1$ ,  $U_a = 1.8$ ,  $U_b = 0.5$ ,  $\gamma_a = 0.15$ ,  $\gamma_b = 0.2$ ,  $\gamma_k = 0.05$ ,  $\varepsilon_a = \varepsilon_a^0 - 0.3$  V,  $\varepsilon_b = \varepsilon_b^0 - 0.1$  V;  $T = 0.2$  (*a*), 0 (*b*). Solid lines correspond to  $\varepsilon_a^\sigma$  and  $\varepsilon_a^{-\sigma}$ . The dotted line shows the mean value of  $\varepsilon_b = (1/2)(\varepsilon_b^\sigma + \varepsilon_b^{-\sigma})$  because atom «*b*» is close to the paramagnetic state for this set of parameters

In the presence of interaction, the  $\varepsilon_a^{-\sigma}(V, n_a^\sigma)$  state filling is suppressed because of a charge redistribution between the two interacting atoms «*a*» and «*b*». Correspondingly, the increase of  $\varepsilon_a^\sigma(V, n_a^{-\sigma})$  and the decrease of  $\varepsilon_a^{-\sigma}(V, n_a^\sigma)$  also are not so fast as in the non-interacting case. Therefore, when atom «*a*» is in the «magnetic» state, the range of the applied bias becomes wider because of the inter-atomic interaction (compare Figs. 4*a* and 4*b*). We stress that this enhancement of the «magnetic» regime is possible only in the nonequilibrium case, i.e., for a nonzero tunneling bias and the energy levels  $\varepsilon_{a(b)}^{\pm\sigma}(V, n_{a(b)}^{\mp\sigma})$  close to the Fermi level of one of the electrodes.

In the equilibrium case, the interaction with paramagnetic atom «*b*» results in the suppression of the «magnetic» state on atom «*a*» (compare Figs. 4*a* and 4*b*).

Figure 5*a, b* depicts the dependence of the tunneling conductivity on the applied bias in the vicinity of

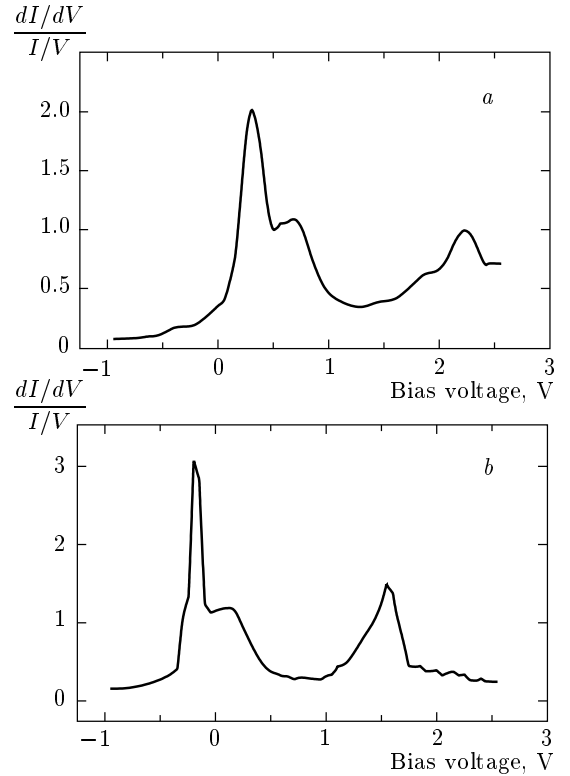


**Fig. 5.** The dependence of the normalized tunneling conductivity on the applied bias voltage for the same sets of parameters as in Fig. 4*a* and *b*

the «*a*» atom. Two broad peaks in the tunneling conductivity spectra correspond to switching «on» the «*a*» atom at

$$\varepsilon_a^\sigma(V, n_a^{-\sigma}) = E_F^t$$

and

$$\varepsilon_a^{-\sigma}(V, n_a^\sigma) = E_F^s.$$

2) For  $\gamma_k \gg \gamma_a, \gamma_b$  (i.e., for a sufficiently strong coupling to the STM tip), the «magnetic» state on the «*a*» atom can appear twice for the opposite polarity. In Fig. 6*a*, the dependence of  $\varepsilon_{a(b)}^{\pm\sigma}(V, n_{a(b)}^{\mp\sigma})$  on the applied bias is shown. In the applied bias range

$$|\varepsilon_a^\sigma(V, n_a^{-\sigma}) - E_F^s| < \Gamma,$$

atom «*a*» is in the «magnetic» state. But as the tunneling bias increases, the filling numbers rapidly decrease and the «magnetic» regime is suppressed, and atom «*a*» can be found in the «paramagnetic» state. However, for the opposite polarity of the applied bias, atom «*a*» can again be found in the «magnetic» state when  $|\varepsilon_a^\sigma(V, n_a^{-\sigma})|$  is close to the Fermi level of the tip,

$$|\varepsilon_a^\sigma(V, n_a^{-\sigma}) - E_F^t| < \Gamma.$$

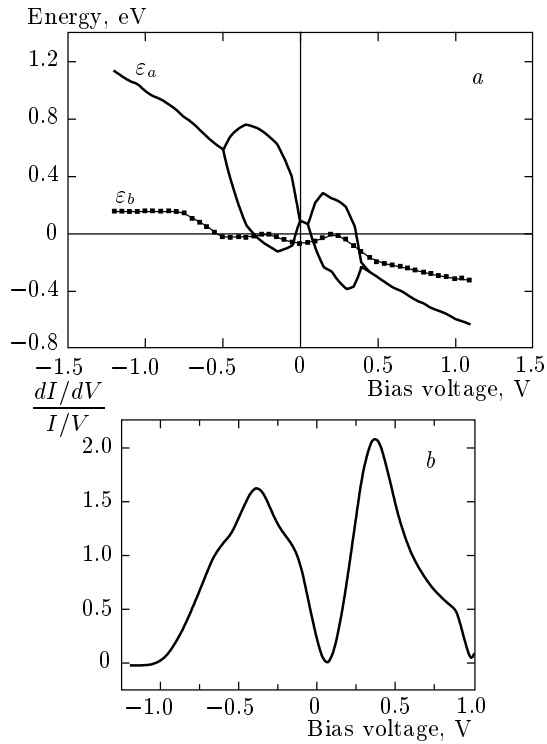


**Fig. 6.** Double switching «on-off» of the magnetic regime of atom «a» for a strong coupling to the STM tip. *a* — The dependence of the «a» and «b» atom energies on the applied bias  $V$ ; the parameters values are (in eV)  $\epsilon_a^0 = -0.7$ ,  $\epsilon_b^0 = -0.5$ ,  $U_a = 2.0$ ,  $U_b = 0.5$ ,  $\gamma_a = 0.05$ ,  $\gamma_b = 0.05$ ,  $\gamma_k = 0.35$ ,  $\epsilon_a = \epsilon_a^0 - 0.3$  V,  $\epsilon_b = \epsilon_b^0 - 0.1$  V;  $T = 0.2$ ; solid lines correspond to  $\epsilon_a^\sigma$  and  $\epsilon_a^{-\sigma}$ ; dotted line shows the mean value of  $\epsilon_b^\sigma$ . *b* — The normalized tunneling conductivity vs. the applied bias voltage

The interaction between the «a» and «b» atoms can enhance this transition. Tunneling conductivity vs. bias voltage is shown in Fig. 6b.

3) Finally, when the coupling to the STM tip is comparable to the coupling of the impurity atom to the substrate, i.e.,  $\gamma_k \geq \gamma_a, \gamma_b$ , increasing the tunneling bias usually leads to the suppression of the «magnetic» state (Fig. 7a) because filling numbers decrease due to the tunneling processes. Figure 7b depicts the suppression of the second maximum of the tunneling conductivity in this case.

Thus, a significant role of the nonequilibrium electron distribution in tunneling processes through coupled Anderson impurities is demonstrated. Tunneling conductivity resonances are sensitive to changes of the electron filling numbers, which are not discrete at a nonzero applied bias. We have shown that an

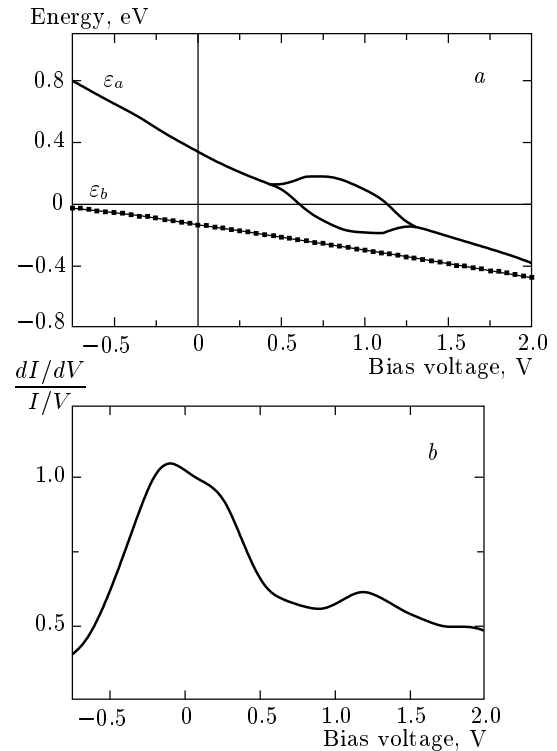


**Fig. 7.** Suppression of the two-fold structure of the tunneling conductivity with the increase of  $\gamma_k$ . *a* — The dependence of the «a» and «b» atom energies on the applied bias  $V$ ; the parameters values are the same as in Fig. 3 except  $\gamma_k = 0.1$ . *b* — The normalized tunneling conductivity vs. the applied bias voltage

impurity atom can be found in the magnetic state for the applied bias within a certain range. Transitions from the paramagnetic regime to the magnetic one and vice versa can occur with changing the bias voltage. In the presence of such transitions, impurity levels can be pinned near the Fermi levels of each electrode, thereby leading to the two-fold structure of spatially resolved tunneling conductivity spectra with enormously broad peaks in the vicinity of each impurity. The theoretical approach proposed here allows us to explain the experimentally obtained STS results and predicts some new interesting possible «switching» regimes. An interesting theoretical prediction is that the interaction between impurities with different values of the Coulomb repulsion can unexpectedly enhance the magnetic regime of a single atom in the nonequilibrium case at a large applied bias. At the same time, the interaction with a «more paramagnetic» neighbor always leads to the suppression of the magnetic state in the equilibrium.

This work was supported in part by the RFBR grants 00-15-96558, 00-15-96555, and 00-02-17759.

### REFERENCES

1. A. Depuydt, C. Van Haesendonck, N. S. Maslova, V. I. Panov, S. V. Savinov, and P. I. Arseev, *Phys. Rev. B* **60**, 2619 (1999).
2. P. I. Arseev, N. S. Maslova, S. I. Oreshkin, V. I. Panov, and S. V. Savinov, *Pis'ma v Zh. Eksp. Teor. Fiz.* **72**, 819 (2000).
3. P. W. Anderson, *Phys. Rev.* **124**, 41 (1961).
4. M. B. Johnson, O. A. Albrektsen, R. M. Feenstra, and H. W. M. Salemnik, *Appl. Phys. Lett.* **63**, 2923 (1993).
5. J. F. Zheng, X. Liu, N. Newman, E. R. Weber, D. F. Ogletree, and M. Salmeran, *Phys. Rev. Lett.* **72**, 1490 (1994).
6. M. C. M. M. Van der Wielen, A. J. A. van Roij, and H. van Kempen, *Phys. Rev. Lett.* **76**, 1075 (1996).
7. Y. Goldin and Y. Avishai, *Phys. Rev. B* **61**, 16750 (2000).
8. A.-P. Jauho, N. S. Wingreen, and Y. Meir, *Phys. Rev. B* **50**, 5528 (1994).
9. J. Konig, T. Pohjola, H. Schoeller, and G. Schon, *Physica E* **6**, 371, (2000).
10. Y. Meir, N. S. Wingreen, and P. A. Lee, *Phys. Rev. Lett.* **66**, 3048 (1991).
11. D. V. Averin, A. N. Korotkov, and K. K. Likharev, *Phys. Rev. B* **44**, 6191 (1991).
12. I. M. Ruzin, V. Chandrasekhar, E. I. Levin, and L. I. Glazman, *Phys. Rev. B* **45**, 13469 (1992).
13. K. Kikoin and Y. Avishai, *Phys. Rev. Lett.* **86**, 2090 (2001).
14. G. D. Mahan, *Many-Particle Physics*, Plenum Press, New York (1990).
15. Y. Goldin and Y. Avishai, *Phys. Rev. Lett.* **81**, 5394 (1998).
16. M. Plihal and J. W. Gadzuk, *Phys. Rev. B* **63**, 85404 (2001).
17. Oded Agam, N. S. Wingreen, and B. L. Altshuler, *Phys. Rev. Lett.* **78**, 1956 (1997).
18. P. I. Arseev, N. S. Maslova, and S. V. Savinov, *Pis'ma v Zh. Eksp. Teor. Fiz.* **68**, 299 (1998).
19. P. I. Arseev and N. S. Maslova, *Zh. Eksp. Teor. Fiz.* **102**, 1056 (1992).
20. F. Hofmann, T. Heinzl, D. A. Wharam et al., *Phys. Rev. B* **51**, 13872 (1995).